NUDT16 and ITPA play a dual protective role in maintaining chromosome stability and cell growth by eliminating dIDP/IDP and dITP/ITP from nucleotide pools in mammals

Abolhassani, Nona
Division of Neurofunctional Genomics, Department of Immunobiology and Neuroscience, Medical Institute of Bioregulation, Kyushu University

Iyama, Teruaki
Division of Neurofunctional Genomics, Department of Immunobiology and Neuroscience, Medical Institute of Bioregulation, Kyushu University

Tsuchimoto, Daisuke
Division of Neurofunctional Genomics, Department of Immunobiology and Neuroscience, Medical Institute of Bioregulation, Kyushu University

Sakumi, Kunihiko
Division of Neurofunctional Genomics, Department of Immunobiology and Neuroscience, Medical Institute of Bioregulation, Kyushu University

他

出版情報：Nucleic Acids Research. 38 (9), pp.2891-2903, 2010-01-15. Oxford University Press
バージョン：

Published online 15 January 2010

Nucleic Acids Research, 2010, Vol. 38, No. 9 ***2891–2903***
doi:10.1093/nar/gkp1250

NUDT16 and ITPA play a dual protective role in maintaining chromosome stability and cell growth by eliminating dIDP/IDP and dITP/ITP from nucleotide pools in mammals

Nona Abolhassani, Teruaki Iyama, Daisuke Tsuchimoto, Kunihiko Sakumi, Mizuki Ohno, Mehrdad Behmanesh and Yusaku Nakabeppu*

Division of Neurofunctional Genomics, Department of Immunobiology and Neuroscience, Medical Institute of Bioregulation, Kyushu University, Fukuoka, 812-8582, Japan

Received November 28, 2009; Revised December 20, 2009; Accepted December 26, 2009

ABSTRACT

Mammalian inosine triphosphatase encoded by *ITPA* gene hydrolyzes ITP and dITP to monophosphates, avoiding their deleterious effects. *Itpa*$^{-}$ mice exhibited perinatal lethality, and significantly higher levels of inosine in cellular RNA and deoxyinosine in nuclear DNA were detected in *Itpa*$^{-}$ embryos than in wild-type embryos. Therefore, we examined the effects of ITPA deficiency on mouse embryonic fibroblasts (MEFs). *Itpa*$^{-}$ primary MEFs lacking ITP-hydrolyzing activity exhibited a prolonged doubling time, increased chromosome abnormalities and accumulation of single-strand breaks in nuclear DNA, compared with primary MEFs prepared from wild-type embryos. However, immortalized *Itpa*$^{-}$ MEFs had neither of these phenotypes and had a significantly higher ITP/IDP-hydrolyzing activity than *Itpa*$^{-}$ embryos or primary MEFs. Mammalian NUDT16 proteins exhibit strong dIDP/IDP-hydrolyzing activity and similarly low levels of *Nudt16* mRNA and protein were detected in primary MEFs derived from both wild-type and *Itpa*$^{-}$ embryos. However, immortalized *Itpa*$^{-}$ MEFs expressed significantly higher levels of *Nudt16* than the wild type. Moreover, introduction of silencing RNAs against *Nudt16* into immortalized *Itpa*$^{-}$ MEFs reproduced ITPA-deficient phenotypes. We thus conclude that NUDT16 and ITPA play a dual protective role for eliminating dIDP/IDP and dITP/ITP from nucleotide pools in mammals.

INTRODUCTION

The accumulation of modified or damaged bases in genomic DNA is a major threat for the alteration of genetic information as a result of mutagenesis or even for programmed cell death. It has been established that such damaged bases in genomic DNA arise from two independent pathways: one is a consequence of the direct modification of the normal bases in the DNA and the other is that of the incorporation of modified nucleotides generated in resident nucleotide pools (1,2).

To control the quality of the nucleotide pools, organisms possess a number of nucleoside triphosphatases, which degrade non-canonical nucleoside triphosphates to the corresponding monophosphates. We had identified and characterized three mammalian enzymes: (i) oxidized purine nucleoside triphosphatase encoded by *MTH1* gene for 8-oxo-2′-deoxyguanosine triphosphate (8-oxo-dGTP), 8-oxoGTP, 2-hydroxy-2′-deoxyadenosine triphosphate (2-OH-dATP) and 2-OH-ATP (3,4); (ii) inosine triphosphatase encoded by *ITPA* gene for deaminated purine nucleoside triphosphates such as 2′-deoxyinosine triphosphate (dITP), ITP and 2′-deoxyxanthosine triphosphate (dXTP) and XTP (5,6); and (iii) a newly discovered enzyme, dCTP pyrophosphatase encoded by *DCTPP1* gene for halogenated dCTPs such as 5-iodo-2′-deoxycytidine triphosphate (7).

To clarify the biological significance of the damaged nucleotides and the enzymes that eliminate them, we had

*To whom correspondence should be addressed. Tel: +81 92 642 6800; Fax: +81 92 642 6791; Email: yusaku@bioreg.kyushu-u.ac.jp
Correspondence may also be addressed to Daisuke Tsuchimoto. Tel: +81 92 642 6802; Fax: +81 92 642 6804;
Email: daisuke@bioreg.kyushu-u.ac.jp
Present addresses:
Mizuki Ohno, Department of Medical Biophysics and Radiation Biology, Faculty of Medical Sciences, Kyushu University, Fukuoka 812-8582, Japan
Mehrdad Behmanesh, Department of Genetics, School of Biological Sciences, Tarbiat Modares University, Tehran, 14115-175, Iran

previously produced and analyzed knockout mice lacking MTH1 or ITPA. *Mth1*$^{-/-}$ mice are viable and survive normally but exhibit an increased incidence of spontaneous tumorigenesis in the liver, stomach and lung (8), while *Itpa*$^{-/-}$ mice die before weaning with features of growth retardation and heart failure (6).

ATP, the most abundant of the nucleotides, plays a fundamental role in a wide variety of cellular processes, including energy transfer, signal transduction, RNA synthesis, cytoskeleton remodeling and muscle contraction. Deamination of adenine at C-6 converts ATP to ITP; such modification is catalyzed by enzymes such as adenosine or AMP deaminase (9), or induced chemically under oxidative stress (7). Because ITP retains a molecular structure similar to that of ATP, it can act as an aberrant substrate replacing ATP in some biological processes (10,11). In the case of cardiac function, a number of sarcomere proteins require ATP for their normal activities. It is likely that during cardiac development in *Itpa*$^{-/-}$ mice the accumulated ITP competes with ATP, which is required for actomyosin function in the sarcomere, thus causing heart failure (6).

Bradshaw and Kuzminov (12) reported that an *Escherichia coli* mutant of *rdgB* gene-encoding inosine triphosphatase has no obvious phenotype; however, the mutant exhibits synergistic lethality in the presence of *recA* or *recBC* mutations. They concluded that RdgB acts to avoid incorporation of 2′-deoxyinosine (dI) in DNA and thereby blocks chromosome fragmentation by hydrolyzing dITP in *E. coli*. These observations strongly suggest that ITPA deficiency in mouse cells also causes chromosomal abnormalities.

In the present study, we examined mouse embryonic fibroblasts (MEFs) prepared from wild-type (*Itpa*$^{+/+}$), *Itpa*$^{+/-}$ and *Itpa*$^{-/-}$ embryos to explore the cellular dysfunction caused by ITPA deficiency. We found that *Itpa*$^{-/-}$ embryos accumulated more than eight times higher levels of dI in nuclear DNA than did wild-type embryos. Moreover, *Itpa*$^{-/-}$ primary MEFs with no ITP-hydrolyzing activity exhibited prolonged doubling times, increased chromosome aberrations and accumulation of single-strand breaks in nuclear DNA. Surprisingly, these phenotypes all disappeared following immortalization of *Itpa*$^{-/-}$ MEFs, with a significant increase in IDP-hydrolyzing activity accompanied by a decreased accumulation of dI in nuclear DNA. We have thus identified a novel enzyme which constitutes a dual enzyme system for eliminating dITP/ITP and dIDP/IDP from nucleotide pools together with ITPA in mammals.

MATERIALS AND METHODS

Nucleotides

Nucleotides used as substrates for enzyme assay were purchased from Sigma-Aldrich (St Louis, MO, USA), or Jena Bioscience GmbH (Jena, Germany). Separation and purification of nucleotides were performed on a Waters Alliance 2690 HPLC separation module (Waters Corp., Milford, MA, USA) equipped with a Model 996 photodiode array detector and a Wakopak Handy ODS column (4.6 × 250 mm) using 100 mM triethyl ammonium hydrogen carbonate solution (pH 7.4) (Wako Pure Chemicals, Osaka, Japan) as the mobile phase. Purified nucleotides were lyophilized five times with solubilization in distilled water.

Itpa gene knockout mice

Itpa gene knockout mice were established as described (6). Genotypes were analyzed using tail DNA. PCR primers used to detect the wild-type and *Itpa* mutant alleles were P46 and P47, or P29 and LNEO1, respectively (Supplementary Table S2). Heterozygous male (*Itpa*$^{+/-}$) were backcrossed with C57BL/6J female (*Itpa*$^{+/+}$) (Clea Japan, Tokyo, Japan) for more than five generations ($N > 5$). All animals were maintained in an air-conditioned, light/time-controlled, specific-pathogen-free room. All studies were approved by the Animal Care and Use Committee, Medical Institute of Bioregulation, Kyushu University.

Preparation of primary and immortalized MEFs

Twenty embryonic gestation day (E)13.5 and E14.5 embryos were obtained by intercross mating of inbred N10 or N11 *Itpa*$^{+/-}$ mice (three pairs). Their genotypes were *Itpa*$^{+/+}$, *Itpa*$^{+/-}$ and *Itpa*$^{-/-}$ at a ratio of 5:10:5. Skin fibroblasts were aseptically isolated from these embryos and at least four independent embryos were used for each genotype (*Itpa*$^{+/+}$, *Itpa*$^{+/-}$, *Itpa*$^{-/-}$). These primary MEFs were cultured in Dulbecco's Modified Eagle's Medium (DMEM) supplemented with 10% heat-inactivated fetal bovine serum (FBS), 100 units/ml penicillin and 100 μg/ml streptomycin at 37°C under 5% CO_2 in air. Primary MEFs in culture were harvested by treatment with 0.15% trypsin–0.08% EDTA in PBS and replated for further passage. Those from Passage 2 were stocked as primary MEFs. Spontaneously immortalized MEFs were established after single colony isolation during 30–40 passages. Their genotypes were determined by genomic polymerase chain reaction (PCR) amplification and three lines of immortalized MEFs were independently established from three embryos for each genotype.

Cell proliferation assays

Primary or immortalized MEFs were seeded at 1×10^5 cells (Figures 1C and 4A) or 0.5×10^5 cells (Figure 7C) per well in six-well plates (Nalge Nunc International K.K., Tokyo, Japan). Cells were harvested every 2 days or every day, respectively, and the numbers of cells were counted using a hemocytometer.

Cell-cycle analysis

Flow cytometric analysis of the cell cycle was performed as described (13). Cells (1×10^6 cells per assay) were centrifuged, washed with phosphate buffered saline (PBS) and suspended in PBS containing 0.2% Triton X-100. We then added 5 μl of RNase A (1 mg/ml) and 50 μl of propidium iodide (PI, 1 mg/ml). DNA content and cell numbers were analyzed with an LSR flow cytometer (Becton Dickinson, San Jose, CA, USA). The

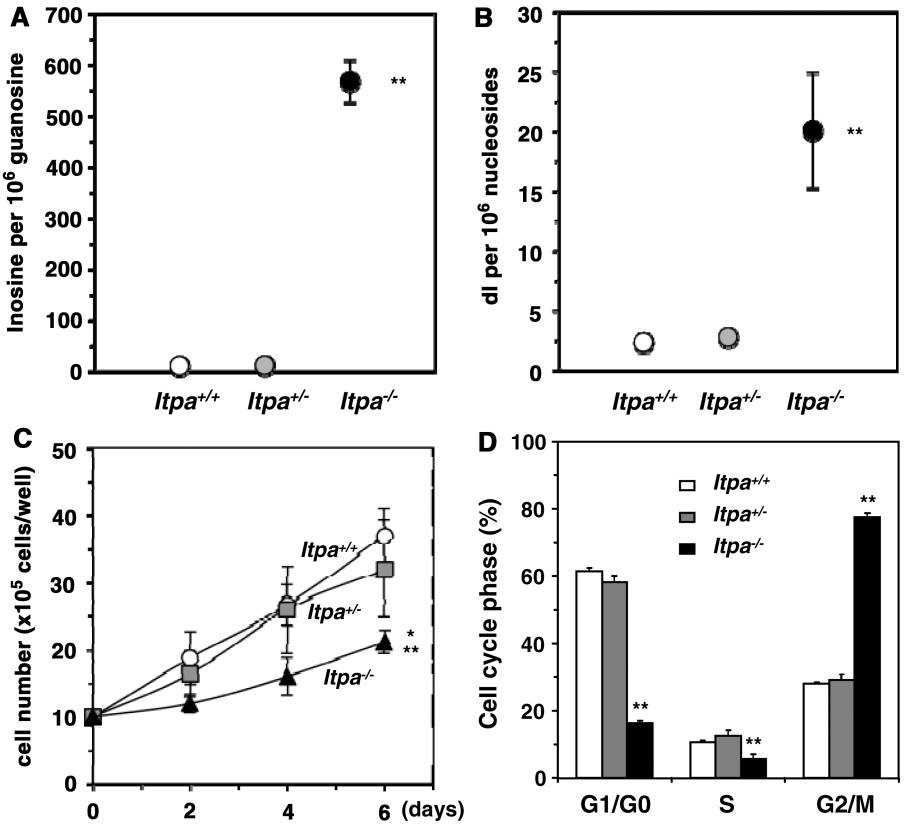

Figure 1. ITPA-deficient primary MEFs exhibit various cellular dysfunctions. (**A**) ITPA deficiency caused a significantly increased accumulation of inosine in cellular RNA. Inosine level was determined by LC–MS/MS analysis of cellular RNA prepared from embryos (N3). Result of non-repeated measures ANOVA (two-tailed), $P = 1.69 \times 10^{-7}$. Student–Newman–Keuls (SNK) *post hoc* test, $^{**}P < 0.01$ (versus $Itpa^{+/+}$ and $Itpa^{+/-}$). Data are shown as the mean ± SD ($n = 3$ independent embryos). (**B**) ITPA deficiency caused a significantly increased accumulation of deoxyinosine (dI) in nuclear DNA. Deoxyinosine (dI) level was determined by LC–MS/MS analysis of nuclear DNA prepared from embryos (N3). Result of non-repeated measures ANOVA (two-tailed), $P = 0.00038$. SNK *post hoc* test, $^{**}P < 0.01$ (versus $Itpa^{+/+}$ and $Itpa^{+/-}$). Data are shown as the mean ± SD ($n = 3$ independent embryos). (**C**) ITPA deficiency impairs normal cell proliferation. Primary MEFs (Passage 2) isolated from four separate $Itpa^{-/-}$ embryos showed significant prolonged doubling time in comparison to those from $Itpa^{+/+}$ and $Itpa^{+/-}$ embryos. Result of repeated measures ANOVA (two-tailed), $P = 0.0005$. Bonferroni/Dunn *post-hoc* test, $^{*}P < 0.05$ (versus $Itpa^{+/-}$), $^{**}P < 0.01$ (versus $Itpa^{+/+}$). Data are shown as the mean ± SD ($n = 4$ independent MEFs). (**D**) ITPA deficiency causes G2/M arrest. Primary MEFs (Passage 5) were subjected to flow cytometry analysis and the percentages of Cell-cycle phases in each MEF set were determined. Result of non-repeated measures ANOVA (two-tailed), $P = 1.74 \times 10^{-8}$. Bonferroni *post hoc* test, $^{**}P < 0.01$ (versus $Itpa^{+/+}$ and $Itpa^{+/-}$). Data are shown as the mean ± SD ($n = 3$ independent isolates).

data were analyzed using CellQuest and ModFit software (Becton Dickinson).

Karyotype analysis

A 50% confluent culture of MEFs was treated with 0.1 μg/ml colcemid (Nacalai Tesque Inc., Kyoto, Japan) for 30 min. After hypotonic treatment of harvested cells in 75 mM KCl, cells were fixed in freshly prepared Carnoy's fixative (methanol:acetic acid 3:1), and the cell suspension was dropped onto a glass slide, air-dried and immediately stained with freshly prepared Giemsa staining solution (Merck KGaA, Darmstadt, Germany cat. no. 1.09204.0509, 25× diluted in PBS) for 20 min. After rinsing the slide in PBS twice and in distilled water twice, air-dried slides were cover-slipped using Permount (Fisher Scientific, Waltham, MA, USA; SP15-100). The slide was observed under an Axioscope 2 plus microscope equipped with AxioCam and AxioVision software (Carl Zeiss MicroImaging Japan, Tokyo, Japan). A total 30 cells in metaphase was examined for each preparation.

Quantification of deoxyinosine or inosine by liquid chromatography coupled with tandem mass spectrometry

The preparation and digestion of nuclear DNA samples were as described (14), except that 10 mM 2, 2, 6, 6-tetramethylpiperidine-*N*-oxyl (TEMPO, Wako Pure Chemicals) and 20 μM 2′-deoxycoformycin (a kind gift from the Chemo-Sero-Therapeutic Research Institute, Kumamoto, Japan), an adenosine deaminase inhibitor, was added at all stages of manipulation, as described by Taghizadeh *et al.* (15). RNA was prepared using RNeasy Mini Kits (Qiagen Inc., Valencia, CA, USA) according to the manufacturer's instructions in the presence of 20 mM TEMPO and 20 μM 2′-deoxycoformycin. DNA or RNA samples were digested with nuclease P1 (Yamasa, Chiba, Japan) and alkaline phosphatase (Sigma-Aldrich, P-5521) and digested samples were subjected to LC–MS/MS

analysis using the Shimadzu VP-10 HPLC system (SHIMADZU CORPORATION, Kyoto Japan) connected to the API3000 MS/MS system (PE-SCIEX, Applied Biosystems, Foster City, CA, USA), as described (14).

Immunostaining

To detect single-stranded (ss) DNA, the slides were incubated with anti-ssDNA (IBL, Takasaki, Japan; code number 18 731, 1/100 dilution) in combination with Alexa Fluor 488-conjugated goat anti-rabbit IgG (Invitrogen, Carlsbad, CA. USA), as described (16). Nuclei were counterstained with 4′, 6-diamino-2-phenylindole (DAPI, 50 ng/ml; Vector, Burlingame, CA, USA). A cover slide was mounted onto the slide with Vectashield (Vector). The slide was observed using an Axioskop 2 plus microscope equipped with AxioCam and AxioVision software (Carl Zeiss MicroImaging Japan). A total of 100 cells were examined for each preparation.

Inosine triphosphatase and Inosine diphosphatase assays

Embryo samples or pellets of immortalized MEFs (1×10^7 cells) were washed twice with PBS and quickly frozen in liquid nitrogen. Frozen samples in 100 µl of lysis buffer containing 50 mM Tris–HCl (pH 8.0), 50 mM NaCl, 1 mM dithiothreitol and protease inhibitor cocktail (Nacalai Tesque), were sonicated at 4°C. The lysate was centrifuged at $17\,360 \times g$ for 60 min and the supernatant was collected as a crude cell extract. The protein concentration was determined with a Protein Assay system (Bio-Rad, Hercules, CA, USA) using bovine serum albumin (Thermo Fisher Scientific Inc., Waltham, MA, USA) as a standard. Inosine triphosphatase or Inosine diphosphatase activities were assayed by measuring the hydrolysis of ITP or IDP to IMP. The reaction mixture contained 50 mM Tris–HCl (pH 8.5), 50 mM $MgCl_2$, 1 mM DTT, 0.2 mM ITP or IDP and 1–10 µg of the crude-cell extract to be examined. The reaction was run at 30°C for 20 min and stopped by adding 150 mM EDTA. The reaction mixture was applied to HPLC analysis as described (6). Separation and quantification of nucleotides were performed by HPLC using a Waters Alliance 2690 separation module equipped with a Model 996 photodiode array detector. A buffer consisting of 75 mM sodium phosphate (pH 6.4), 0.4 mM EDTA, with 20% acetonitrile was used as the mobile phase in a TSK-GEL DEAE-2SW column, 4.6 × 250 mm (Tosoh Corp., Tokyo, Japan).

Quantitative real-time reverse transcription polymerase chain reaction

MEFs were seeded at 1×10^5 cells per well with 500 µl of medium in 24-well plates and cultured to 70–80% confluency, or for 3 days. RNA was extracted from the harvested cells using an Isogen kit (Nippon Gene Inc., Tokyo, Japan). Totally 2 µg of total RNA was subjected to RNase-free DNase I treatment and cDNA synthesis using random decamers and a Cells-to-cDNA II kit (Ambion), according to the manufacturer's instructions. Quantitative real-time PCR was performed using an ABI Prism 7000 sequence detection system with 10 ng cDNA, a set of *Nudt16* primers (FmNud3RT, RmNud3RT; 200 nM) or a set of *Gapdh* primers (F-Gapdh, R-Gapdh; 50 nM) and Power SYBR Green PCR Master Mix (Applied Biosystems) in a total volume of 25 µl. The PCR reaction was performed as follows: a single cycle of 50°C for 2 min, a single cycle of 95°C for 10 min, followed by 40 cycles of 95°C for 15 s and 60°C for 1 min. The primers were designed using PRIMER EXPRESS software (Applied Biosystems) and their sequences are shown in Supplementary Table S2. Specificity of the PCR products was established by dissociating curve analysis and by running the products on a 2% agarose gel to verify their size. The *Nudt16* mRNA level is expressed relative to the *Gapdh* mRNA level. Serially diluted cDNA was used to obtain a standard curve for each transcript.

Western blotting

MEFs were seeded at 5×10^5 cells per dish in 10 ml medium in a 90 mm Petri dish (Nalge Nunc International K.K.) and were cultured to 70–80% confluency or for 3 days. Cells were washed twice with PBS and harvested using 2× SDS sample buffer [125 mM Tris–HCl (pH 6.8), 4% SDS, 10% glycerol, 4% 2-mercaptoethanol]. The protein concentration was determined using a Protein Assay system as above. Protein samples were separated by SDS–PAGE and transferred to 0.45 µm Immobilon-P membrane (Millipore Inc., Madison, WI, USA) and western blot analysis using anti-hNUDT16 (1 µg/ml) or anti-ITPA antiserum (1/500 dilution) (5) with horseradish peroxidase-conjugated protein A and an ECL-Plus kit (GE Healthcare Bio-Sciences, Piscataway, NJ, USA) was performed as described (17). The same membrane was treated with WB stripping solution (Nacalai Tesque) and reprobed with anti-GAPDH (Millipore, Inc., Billerica, MA, USA; MAB374, 10^5× diluted) and HRP-anti-mouse IgG (BD Biosciences, San Jose, CA, USA).

Expression of recombinant mouse NUDT16 protein

An expression vector for the mouse NUDT16 protein was constructed by inserting the NdeI-HindIII fragment of pET28a(+):mNudt16 into the NdeI-HindIII region of pET32a(+) (Merck KGaA), thus Trx·Tag-His·Tag-S·Tag sequences were removed. *Escherichia coli* BL21 cells were transfected with pET32a(+) vector or pET32a:mNudt16 using a Cell-porator (Life Technologies, Carlsbad, CA, USA) according to the manufacturer's instructions. Transformants were selected on LB-agar plates in the presence of 30 µg/ml ampicillin. Established transformants were cultured until the OD_{600} reached 0.6 and then incubated with 1 mM isopropyl β-D-thiogalactoside for a further 3 h. Cells were harvested by centrifugation and resuspended in 1 ml of 2× SDS sample buffer. Samples were subjected to 12.5% SDS–PAGE and the expression of mouse NUDT16 protein without tag was confirmed by western blotting.

Introduction of silencing RNA into immortalized MEFs

Nudt16 siRNA (Ambion/Applied Biosystems, Austin, TX, USA; *Silencer* Select; s93780, s93782, 25 μM) or control siRNA (Ambion/Applied Biosystems, *Silencer* Select Negative Control #1 siRNA, cat. no. 4390844) was introduced into immortalized MEFs ($Itpa^{+/+}$, $Itpa^{-/-}$) by electroporation using a MicroPorator-mini (Digital Bio Technology, Seoul, Korea, MP-100, 1100 V, 10 ms for 2 pulses) and cells were replated appropriately into six-well plates 1 day after electroporation for further analysis.

Statistical analysis

Statistical analysis was performed using Stat View 5.0 (SAS Institute Inc., Cary, NC, USA). The statistical significance between two groups was determined with Student's *t*-test, and that among more than three groups was determined with non-repeated or repeated measures ANOVA with an appropriate correction for multiple comparisons as described in each figure legend. *P*-values <0.05 are considered statistically significant.

RESULTS

ITPA deficient primary MEFs exhibit various cellular dysfunctions

$Itpa^{-/-}$ mice with a 129·C57BL/6J mixed genetic background exhibited incomplete embryonic lethality and the surviving pups die about 2 weeks after birth with growth retardation and heart failure (6). After backcrossing the heterozygotes ($Itpa^{+/-}$) to C57BL/6J mice for more than five generations (N5), intercrosses of the obtained $Itpa^{+/-}$ mice yielded $Itpa^{-/-}$ embryos in uterus in accordance with Mendel's laws until embryonic gestation day (E) 18, but there were few newborn pups (Supplementary Table S1), indicating that ITPA deficiency causes perinatal lethality in a C57BL/6J genetic background.

We confirmed significantly increased accumulation of inosine (567.3 ± 41.4 residues per 10^6 guanosine) in cellular RNA prepared from $Itpa^{-/-}$ embryos (N14) in comparison to those from $Itpa^{+/+}$ (10.5 ± 1.50) and $Itpa^{+/-}$ (11.4 ± 1.07) embryos by liquid chromatography coupled with tandem mass spectrometry (LC–MS/MS) analysis (Figure 1A), as previously observed in various tissues of surviving $Itpa^{-/-}$ pups (6).

Furthermore, LC–MS/MS analysis of nuclear DNA prepared from embryos revealed that $Itpa^{-/-}$ embryos (E14.5) obtained from intercrosses of $Itpa^{+/-}$ mice (N3) contained significantly more dI in their nuclear DNA (20.1 ± 4.8 residues per 10^6 nucleosides): more than eight times that measured in $Itpa^{+/+}$ embryos (2.34 ± 0.76) (Figure 1B). The increased dI levels were also confirmed in $Itpa^{-/-}$ embryos after further backcrossing to C57BL/6J mice (N14, E13.5, 24.5 ± 2.24 dI residues per 10^6 nucleosides).

To examine the nature of the cellular dysfunction caused by ITPA deficiency, we isolated embryos (at E13.5 and E14.5) from intercrosses of $Itpa^{+/-}$ littermates (N10, one pair; N11, two pairs) and determined their genotypes (Supplementary Table S1). Among 20 embryos, five were found to be $Itpa^{-/-}$, 10 were $Itpa^{+/-}$ and the remaining five were $Itpa^{+/+}$. Then we isolated primary MEFs independently from four embryos of each genotype and their genotypes and the expression levels of ITPA protein were confirmed (Supplementary Figure S1A and B). All $Itpa^{-/-}$ primary MEFs at the second passage showed significantly longer doubling time (132.0 ± 14.6 h) than those from $Itpa^{+/+}$ (78.6 ± 10.1 h) and $Itpa^{+/-}$ (87.5 ± 14.3 h) embryos (Figure 1C). There was no obvious difference in their morphology under phase contrast microscopy (Supplementary Figure S1C). In Passage 5, we observed essentially the same proliferation deficiency in $Itpa^{-/-}$ MEFs and slightly increased numbers of senescence-associated β-galactosidase (SA-β-Gal)-positive cells in $Itpa^{-/-}$ MEFs ($Itpa^{+/+}$ versus $Itpa^{-/-}$, 3.64% versus 7.74%; Supplementary Figure S2A and B). Flow cytometry analysis of the cell cycle revealed that $Itpa^{-/-}$ MEFs exhibited a significant increase in the G2/M phase ($Itpa^{+/+}$ versus $Itpa^{-/-}$, 28.4% versus 77.4%; Figure 1D) and a slight increase in the sub G1 fraction ($Itpa^{+/+}$ versus $Itpa^{-/-}$, 1.61% versus 5.51%; fraction M1 in Figure 2A). There was an apparent increase in cells with an abnormally increased DNA content in $Itpa^{-/-}$ MEFs compared with $Itpa^{+/+}$ MEFs (fraction M3 in Figure 2A), indicating that the G2/M phase shown in Figure 1D might have contained some tetraploid cells at the G1 phase (Figure 2B). There was no increase in dead cells detected as propidium iodide (PI)/Hoechst-double positive cells (Supplementary Figure S2C). These results indicate that ITPA deficiency caused delay or arrest in cell-cycle progression. We further observed that exposure of $Itpa^{-/-}$, but not $Itpa^{+/+}$, $Itpa^{+/-}$ MEFs, to sodium nitrite ($NaNO_2$), which causes predominant deamination of purine bases (18), resulted in growth suppression without inducing cell death (Supplementary Figure S2C).

We next examined for chromosomal abnormalities in mitotic cells (Figure 3A). As shown in Figure 3B, chromosomal structural abnormalities were more frequently observed in $Itpa^{-/-}$ MEFs than in $Itpa^{+/+}$ MEFs, especially premature centromere separation (3.33 times more common), chromatid gaps (2.04 times) and chromatid breakages (1.52 times). Moreover, the percentage of cells with abnormal chromosomes in $Itpa^{-/-}$ primary MEFs was significantly higher than among $Itpa^{+/+}$ and $Itpa^{+/-}$ MEFs. There was an increase in ploidy abnormalities among $Itpa^{-/-}$ primary MEFs (Figure 2B): thus 41.2% in the mitotic fraction exhibited tetraploidy, while about 25% of mitotic fractions in $Itpa^{+/+}$ and $Itpa^{+/-}$ MEFs were detected as tetraploids. This confirmed the increase in ploidy among $Itpa^{-/-}$ MEFs.

Because chromatid gaps or breakages are most likely to be caused by the accumulation of single- or double-strand breaks in DNA, we examined levels of single-strand breaks (SSBs) in DNA using an antibody against single-stranded (ss) DNA (anti-ssDNA) (Figure 3C) (16). Immunofluorescence microscopy with anti-ssDNA revealed that the percentages of immunoreactive nuclei in $Itpa^{-/-}$ primary MEFs were significantly higher than in $Itpa^{+/+}$ MEFs (Figure 3D). Thus, more SSBs

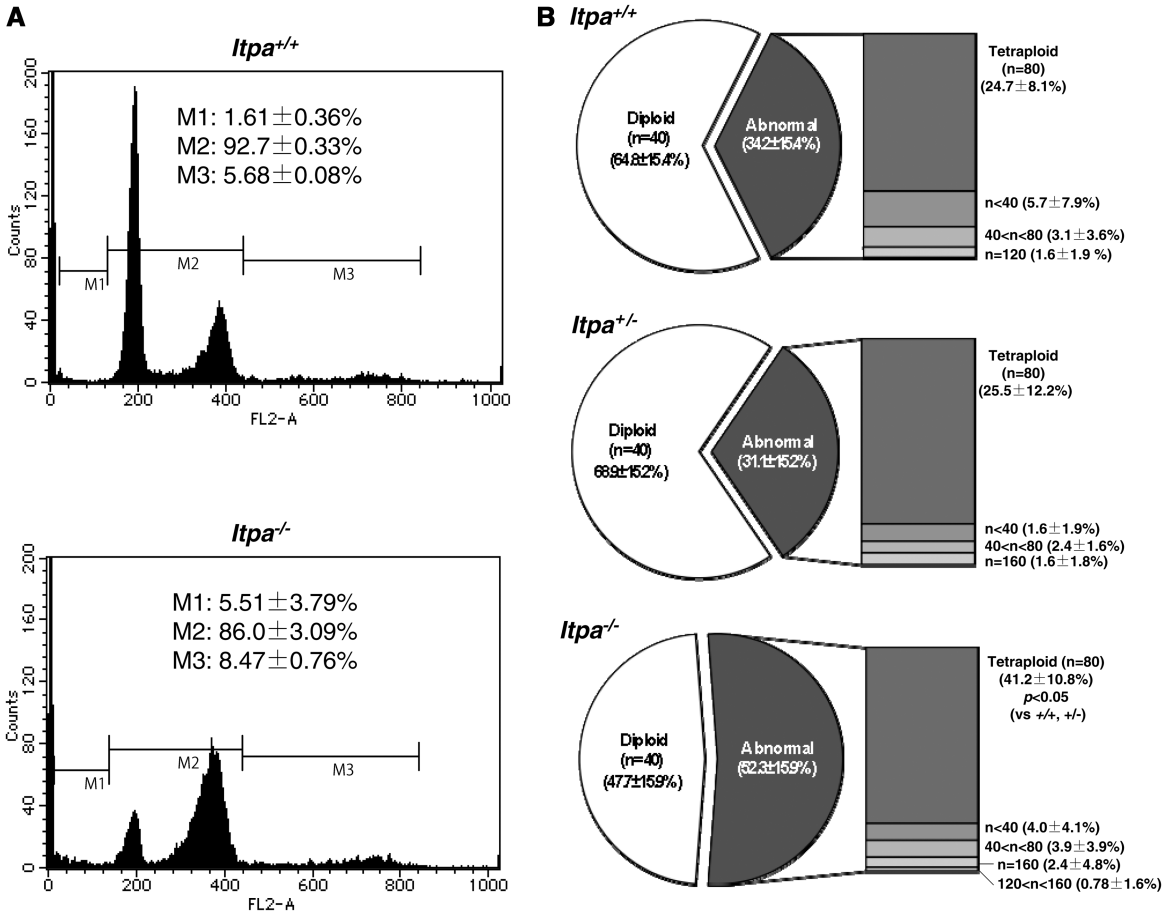

Figure 2. Increased DNA content in ITPA deficient primary MEFs. (**A**) Flow cytometric analysis of the cell cycle was performed and the sub G1 fraction (M1), diploid fraction (M2) and a fraction with an increased DNA content (M3) were determined. (**B**) ITPA deficiency increased chromosomal ploidy in primary MEFs. Percentages of diploid, tetraploid and others are shown in pie charts with the mean ± SD (three independent isolates). The frequency of tetraploidy was increased significantly in $Itpa^{-/-}$ MEFs. Results show non-repeated measures ANOVA (two-tailed): $P = 0.094$. *P*-value is shown following a Bonferroni *post hoc* test.

had accumulated in the DNA of $Itpa^{-/-}$ primary MEFs. Furthermore, the nuclei were heterogeneous in $Itpa^{-/-}$ MEFs and both the small and large nuclei exhibited ssDNA immunoreactivity (Figure 3C).

Immortalization of $Itpa^{-/-}$ MEFs reversed the ITPA-deficient phenotypes with increased ITP/IDP-hydrolyzing activity

To obtain established cell lines with ITPA deficiency, spontaneously-immortalized MEFs were isolated after 30–40 passages of each primary MEF line. We noticed that each immortalized MEF population showed the same proliferation rate, irrespective of their genotype (Figure 4A). The extent of chromosomal abnormalities (Figure 4B), and both levels of dI (2.49 ± 0.24 dI residues per 10^6 nucleosides) and ssDNA (positive in $6.17 \pm 0.68\%$ of cells) in nuclear DNA (Figure 7E and F) were similarly decreased in immortalized $Itpa^{-/-}$ MEFs. Furthermore, the G1 phase fraction increased significantly in immortalized $Itpa^{-/-}$ MEFs (Figure 5A) compared with primary MEFs (Figure 2A). Because the percentages of tetraploids were significantly higher in both primary and immortalized $Itpa^{-/-}$ MEFs than $Itpa^{+/+}$ or $Itpa^{+/-}$ MEFs (Figures 2B and 5B), the G2/M fraction in immortalized $Itpa^{-/-}$ MEFs was apparently less than in primary $Itpa^{-/-}$ MEFs.

To test whether any backup enzyme for ITPA deficiency might exist in the immortalized $Itpa^{-/-}$ MEFs, we measured ITP-hydrolyzing activity in extracts prepared from embryos and immortalized MEFs (Table 1, Supplementary Figure S3). There was no detectable ITP-hydrolyzing activity in extracts prepared from $Itpa^{-/-}$ embryos, but a significantly high rate was detected in $Itpa^{+/+}$ embryos, thus confirming ITPA deficiency in $Itpa^{-/-}$ embryos. We also confirmed that $Itpa^{-/-}$ primary MEFs (Passage 3) did not generate IMP from ITP. On the other hand, we detected substantial activity in extracts from immortalized $Itpa^{-/-}$ MEFs, although the levels were less than 20% of that detected in immortalized $Itpa^{+/+}$ MEFs or embryos. We then measured IDP-hydrolyzing activity in these extracts (Table 1, Supplementary Figure S3). Levels were increased both in $Itpa^{+/+}$ and $Itpa^{-/-}$ MEFs during immortalization and the activity was more significantly increased in immortalized $Itpa^{-/-}$ MEFs than in immortalized $Itpa^{+/+}$ MEFs. These results strongly suggest that an increased

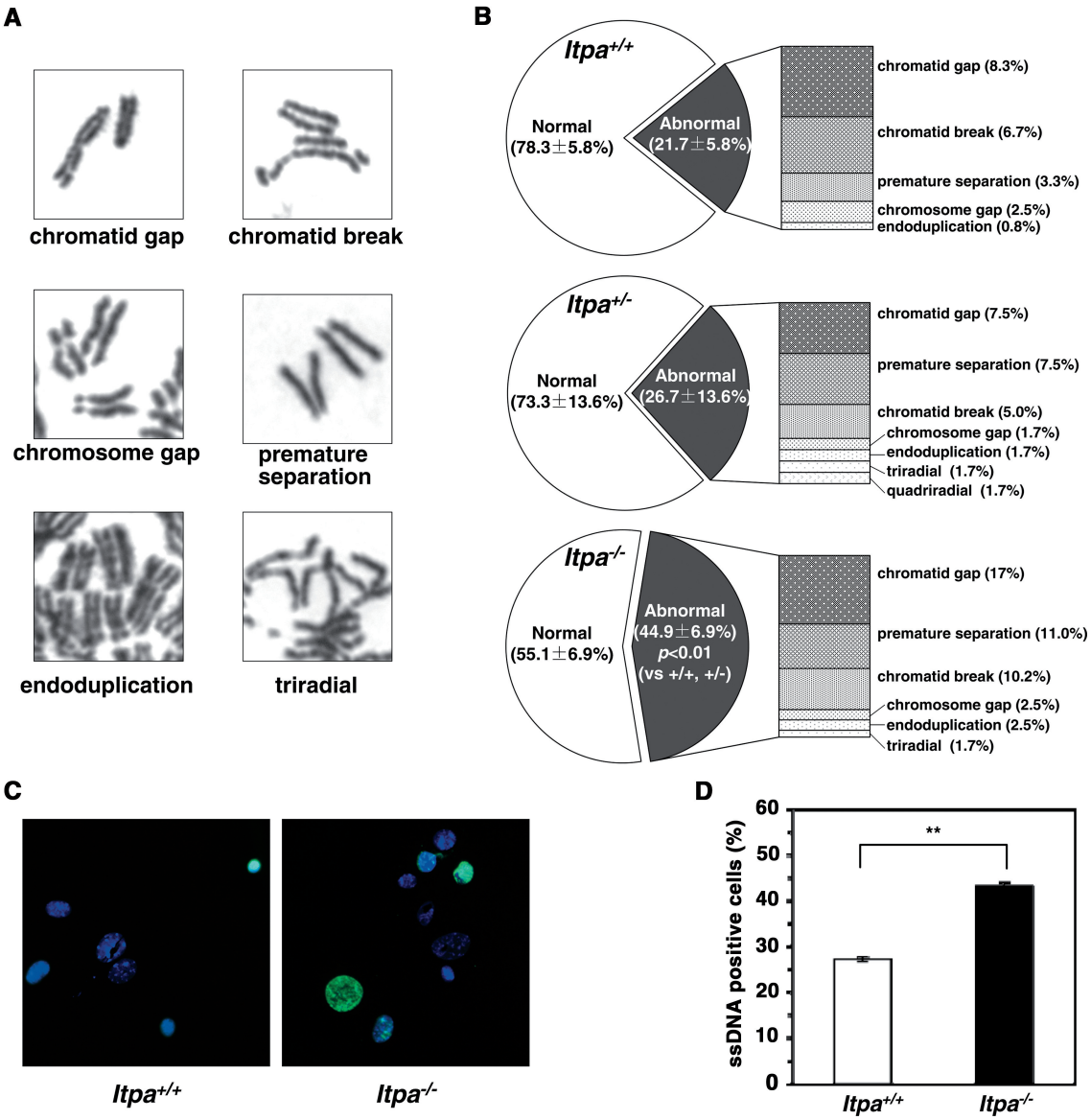

Figure 3. ITPA deficiency increases chromosome abnormalities with increased accumulation of SSBs in nuclear DNA. (**A**) Various chromosome structural abnormalities were observed in *Itpa*$^{-/-}$ primary MEFs (Passage 2). (**B**) ITPA deficiency increases chromosome abnormalities. The frequency of chromosomal abnormality was significantly increased in *Itpa*$^{-/-}$ MEFs in comparison to *Itpa*$^{+/+}$ and *Itpa*$^{+/-}$ MEFs. Result of non-repeated measures ANOVA (two-tailed), $P = 0.0149$. Bonferroni *post hoc* test, $P < 0.01$. Data are shown as pie charts with the mean ± SD ($n = 4$ independent isolates). (**C**) Detection of immunoreactivity against ssDNA in *Itpa*$^{-/-}$ primary MEFs. Immunofluorescence microscopy with anti-ssDNA antibody (green) revealed significantly increased ssDNA immunoreactivity in nuclei (DAPI, blue) of *Itpa*$^{-/-}$ primary MEFs (Passage 2) compared with the wild-type (*Itpa*$^{+/+}$). (**D**) Significant Increase in the ssDNA-positive population in *Itpa*$^{-/-}$ primary MEF tested by unpaired Student's *t*-test (two-tailed): $^{**}P < 0.01$. Data are shown in a bar graph (mean ± SD, $n = 4$ independent isolates).

expression of IDP or ITP-hydrolyzing enzyme(s) blocked or reversed the ITPA-deficient phenotypes observed in primary *Itpa*$^{-/-}$ MEFs.

NUDT16 with strong (deoxy)inosine diphosphatase activity is responsible for cancellation of ITPA-deficient phenotypes and an increase in ITP/IDP-hydrolyzing activity during immortalization

We recently found that the human NUDT16 (nudix [nucleoside diphosphate linked moiety X]-type motif 16) protein, identified as an ITP/XTP/GTP binding protein, has strong IDP and 2′-deoxy-IDP (dIDP)-hydrolyzing activities with weak ITP/dITP-hydrolyzing activities. We also confirmed that mouse NUDT16 protein has essentially the same activities as the human protein (Iyama *et al.*, in preparation). Therefore, we compared *Nudt16* mRNA levels among primary and immortalized *Itpa*$^{+/+}$ or *Itpa*$^{-/-}$ MEFs (Figure 6A). Quantitative real-time reverse transcription polymerase chain reaction (RT–PCR) analysis revealed that the expression levels of *Nudt16* mRNA were similar between primary MEFs derived from *Itpa*$^{+/+}$ and *Itpa*$^{-/-}$ embryos. In contrast, the expression levels of *Nudt16* mRNA in immortalized *Itpa*$^{-/-}$ MEFs were more than 3-fold higher than those of primary *Itpa*$^{-/-}$ MEFs and more than 2-fold higher

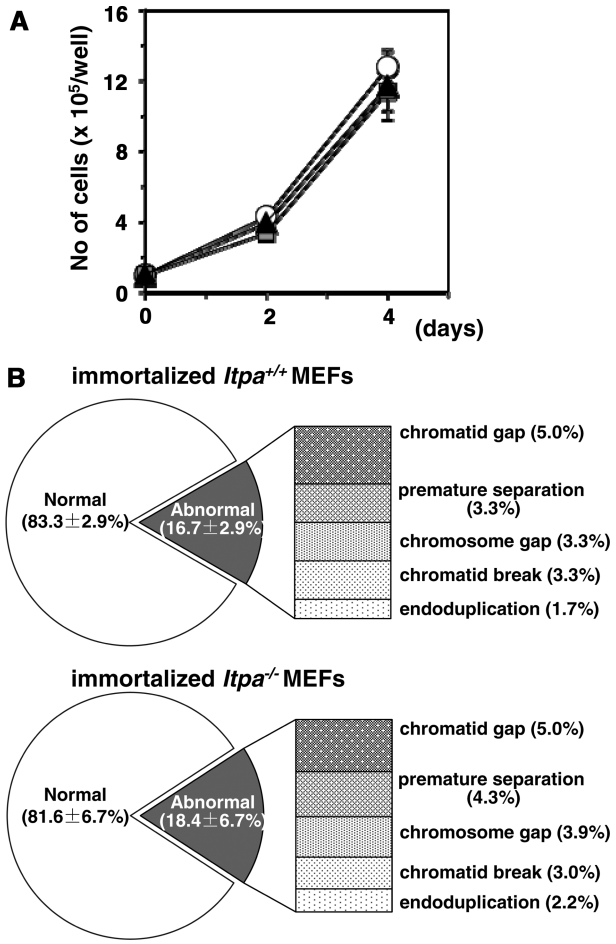

Figure 4. ITPA-deficient phenotypes are reversed during immortalization. (**A**) Immortalized *Itpa*$^{-/-}$ MEFs (triangle) showed the same proliferation rate as did immortalized *Itpa*$^{+/+}$ (circle) and *Itpa*$^{+/-}$ (square) MEFs. Error bars represent the SD ($n = 3$ independent isolates). (**B**) The frequency of chromosomal abnormalities was decreased in immortalized *Itpa*$^{-/-}$ MEFs to the levels seen in immortalized *Itpa*$^{+/+}$ MEFs. Data are shown as the mean ± SD ($n = 3$ independent isolates).

than those in immortalized *Itpa*$^{+/+}$ MEFs (Figure 6A). Significantly increased expression of NUDT16 protein in immortalized *Itpa*$^{-/-}$ MEFs was confirmed by western blotting analysis of crude cell extracts prepared from these MEFs (Figure 6B). We thus conclude that the increased expression of *Nudt16* in immortalized *Itpa*$^{-/-}$ MEFs is responsible for the increase in ITP/IDP-hydrolyzing activity compared with immortalized *Itpa*$^{+/+}$ MEFs.

To examine the contribution of NUDT16 to the reversal of ITPA-deficient phenotypes in immortalized *Itpa*$^{-/-}$ MEFs, knockdown of *Nudt16* mRNA expression was performed using a mixture of two different *Nudt16* silencing (si)RNAs. This treatment caused an efficient reduction of both *Nudt16* mRNA and protein levels to less than 20% of the levels seen in controls (Figure 7A and B). Knockdown of *Nudt16* expression in immortalized *Itpa*$^{-/-}$ but not in *Itpa*$^{+/+}$ MEFs caused a significant reduction in proliferation rate (Figure 7C), as observed in primary *Itpa*$^{-/-}$ MEFs (Figure 1C).

We next measured inosine levels in cellular RNA with or without *Nudt16* siRNAs. Immortalized *Itpa*$^{-/-}$ MEFs contained 516.8 ± 22.3 inosine residues per 10^6 guanosine residues of RNA in the presence of control siRNA which was slightly lower than that in *Itpa*$^{-/-}$ embryos (567.3 ± 41.4 residues per 10^6 guanosine), and *Nudt16* expression knockdown increased the level to 648.5 ± 01.7 residues per 10^6 guanosine residues of RNA (Figure 7D). As shown in Figure 7E, immortalized *Itpa*$^{-/-}$ MEFs contained 2.49 ± 0.24 dI residues per 10^6 nucleosides in nuclear DNA in the presence of control siRNA which was equivalent to that in immortalized *Itpa*$^{+/+}$ MEFs (2.74 ± 0.17 dI residues per 10^6 nucleosides). *Nudt16* expression knockdown in immortalized *Itpa*$^{-/-}$ MEFs significantly increased the level more than 5-fold (12.73 ± 0.99 residues per 10^6 nucleosides). In contrast, knockdown of *Nudt16* expression in immortalized *Itpa*$^{+/+}$ MEFs did not affect the level of dI accumulation in nuclear DNA (2.96 ± 0.3 dI residues per 10^6 nucleosides).

Knockdown of *Nudt16* expression significantly increased the immunoreactivity against ssDNA in immortalized *Itpa*$^{-/-}$ MEFs (Figure 7F). Moreover, karyotyping of immortalized *Itpa*$^{-/-}$ MEFs after *Nudt16* expression knockdown revealed a significant increase in chromosome structural abnormalities, such as chromatid gaps, premature separation and triradial forms compared with controls (Figure 7G).

Thus, increased expression of *Nudt16* was responsible for reversal of the ITPA-deficient phenotypes with reduction of dI accumulation in nuclear DNA but not inosine in cellular RNA.

DISCUSSION

ITPA deficiency increases the accumulation of deoxyinosine in nuclear DNA resulting in severe cellular dysfunction

Here, we showed for the first time that ITPA deficiency caused a significant accumulation of dI in the nuclear DNA of mouse embryos, most of which are likely to die around the time of birth. In wild-type embryos, fewer than three residues of dI per 10^6 nucleosides, corresponding to about 20 000 residues in a whole cell, were detected in nuclear DNA, whereas about 20 residues of dI per 10^6 nucleosides reaching more than 10^5 residues per cell accumulated in *Itpa*$^{-/-}$ embryos. These results indicate that both spontaneous generation of dITP and incorporation of dITP into DNA occurred at significantly high frequencies. Thus, ITPA deficiency caused severe cellular dysfunction resulting in perinatal lethality. Indeed, we demonstrated that this deficiency in primary MEFs increased the accumulation of SSBs in nuclear DNA detected as ssDNA immunoreactivity and as chromosomal abnormalities such as chromatid/chromosome gaps or breaks. There was also premature centromere separation. All these chromosomal anomalies are likely to cause G2/M arrest thus suppressing cell proliferation, as observed in primary *Itpa*$^{-/-}$ MEFs.

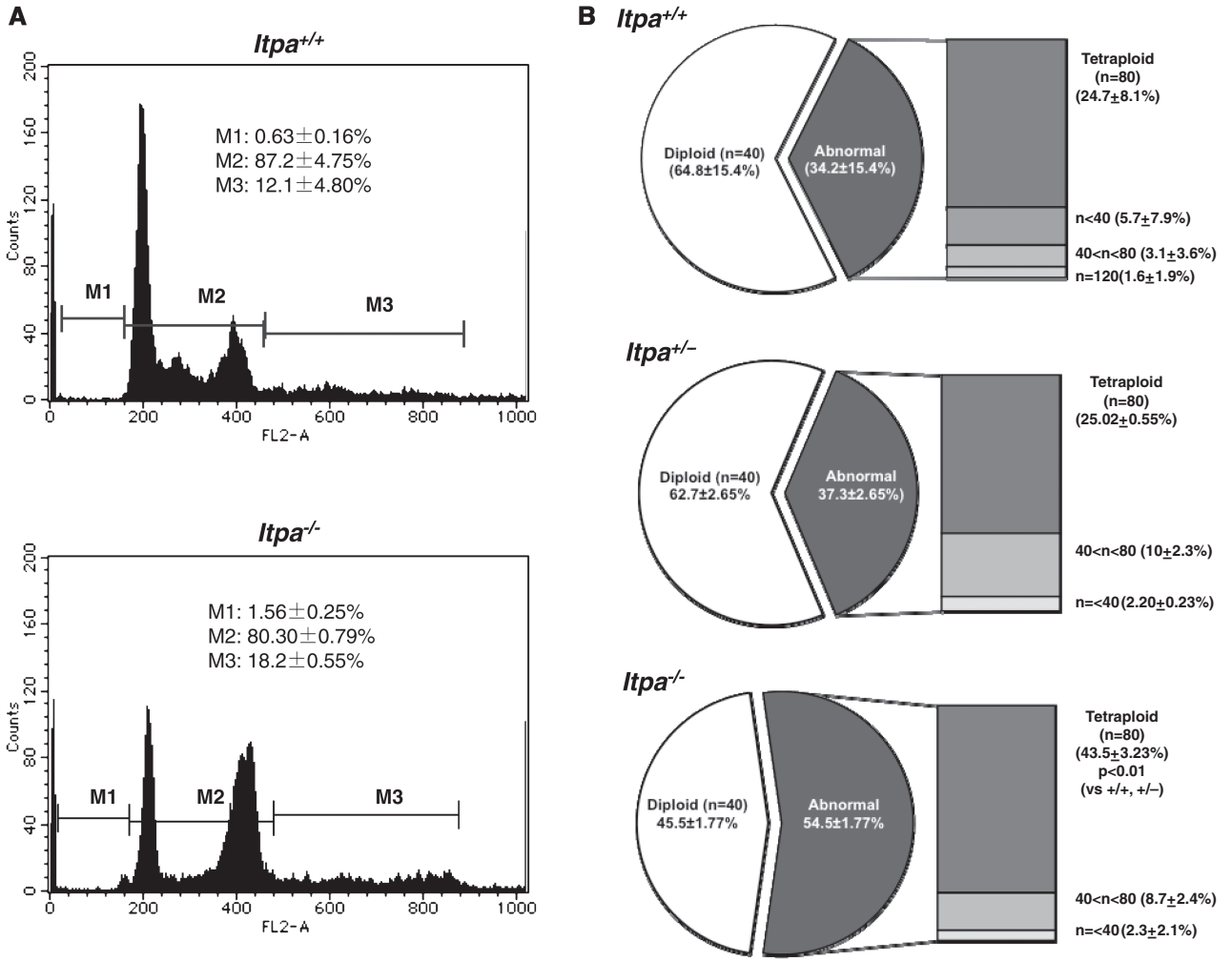

Figure 5. Increased DNA content in ITPA deficient immortalized MEFs. (**A**) Flow cytometric analysis of the cell cycle was performed and the sub G1 fraction (M1), diploid fraction (M2) and a fraction with an increased DNA content (M3) were determined. (**B**) ITPA deficiency increased chromosomal ploidy in immortalized MEFs. Percentages of diploid, tetraploid and others are shown in pie charts with the mean ± SD (three independent isolates). The frequency of tetraploidy was increased significantly in $Itpa^{-/-}$ MEFs. Results show non-repeated measures ANOVA (two-tailed): $P = 0.00015$. *P*-values are shown following a Bonferroni *post hoc* test.

Table 1. Specific ITP/IDP hydrolysis activity in crude-cell extracts prepared from embryos and immortalized MEFs

Cell extract	Substrate	Isolate no. 1		Isolate no. 2	
		Specific activity (u/μg)	SD	Specific activity (u/μg)	SD
$Itpa^{+/+}$ embryo	ITP	6.34	0.8	4.08	0.7
$Itpa^{+/+}$ embryo	IDP	0.84	0.2	1.26	0.4
$Itpa^{+/+}$ iMEF	ITP	6.42	0.9	7.24	1.0
$Itpa^{+/+}$ iMEF	IDP	3.49	0.5	3.68	0.4
$Itpa^{-/-}$ embryo	ITP	ND		ND	
$Itpa^{-/-}$ embryo	IDP	0.86	0.3	1.85	0.4
$Itpa^{-/-}$ iMEF	ITP	1.09	0.1	1.36	0.3
$Itpa^{-/-}$ iMEF	IDP	5.90	0.5	7.85	1.5

As a measure,1 unit (u) was defined as the level of activity producing 1 pmol of IMP at 30°C for 1 min with 0.2 mM ITP/IDP, pH = 8.0, $n = 3$. Key: ND, not detected; iMEFs, immortalized MEFs.

In *E. coli*, the lethality of *rdgB recA* or *rdgB recBC* double mutants, the former-encoding inosine triphosphatase, is suppressed by the inactivation of endonuclease V (EndoV) (12), which cleaves at the second phosphodiester bond at 3′ to dI and initiates nucleotide excision repair (19). It is likely that an inosine triphosphatase deficiency in *E. coli* results in the accumulation of its substrate nucleotides, dITP in the nucleotide pools, thus causing an increased accumulation of dI into DNA. Further excision repair initiated by EndoV leads to chromosomal fragmentation in *recA* or *recBC* mutants.

In mammals, there are at least two enzymes that might be involved in excision repair of dI: the mammalian homolog of EndoV and alkyladenine DNA glycosylase (AAG) which can excise hypoxanthine, a deaminated adenine base (20–24). Because mammalian cells are likely to be less efficient in recombination repair than *E. coli* (25), ITPA deficiency itself thus causes severe

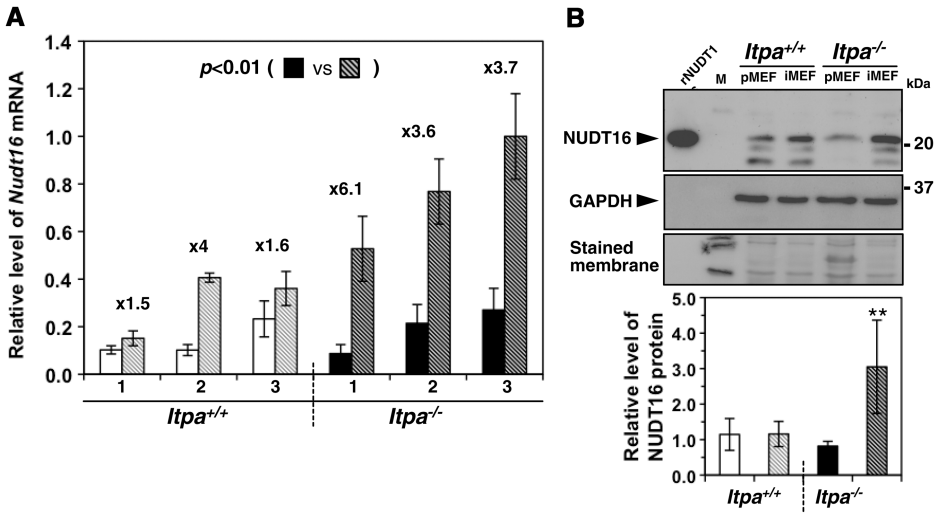

Figure 6. NUDT16 with strong dIDP/IDP-hydrolyzing activity is the back-up enzyme responsible for the cancellation of ITPA-deficient phenotypes during immortalization. (**A**) Expression of *Nudt16* mRNA. Quantitative real-time RT–PCR was performed to compare *Nudt16* mRNA levels between primary (passage 3) and immortalized MEFs. Levels of *Nudt16* mRNA were normalized to those of *Gapdh* mRNA. Values relative to the highest level of *Nudt16* mRNA in immortalized *Itpa*$^{-/-}$ MEFs (isolate No. 3) are shown. Unpaired Student's *t*-test (two-tailed) showed $P < 0.01$ between primary and immortalized *Itpa*$^{-/-}$ MEFs. Data are shown in a bar graph (mean ± SD), with fold changes between primary and immortalized MEFs ($n = 3$ independent isolates). Open and black bars show primary MEFs; shaded bars indicate immortalized MEFs. (**B**) Expression of NUDT16 protein. Western blotting was performed for crude cell extracts (40 μg) prepared from primary (Passage 2) and immortalized MEFs, using anti-NUDT16 antibody (top). GAPDH was detected as an internal control (middle). Membranes were stained with Gel Code Blue in order to confirm the loading and transfer (bottom). Intensities of NUDT16 bands were measured and relative levels normalized to GAPDH are shown in a bar graph. Open and black bars show primary MEFs; shaded bars indicate immortalized MEFs. Result of non-repeated measures ANOVA (two-tailed), $P < 0.019$. Bonferroni *post hoc* test, $^{**}P < 0.01$ (versus others). Error bars represent the SD ($n = 3$ independent isolates).

phenotypes with massive generation of SSBs in DNA, likely caused by efficient excision repair of dI or hypoxanthine.

In primary *Itpa*$^{-/-}$ MEFs, increased frequency of chromosomal abnormalities such as chromatid/chromosome gaps or breaks might result from increased SSB accumulation in nuclear DNA, which is likely to be caused by excision repair of accumulated dI in nuclear DNA. It is noteworthy that exposure of peripheral lymphocytes to ITP or IDP in culture were reported to cause chromosome aberrations such as chromatid breaks and gaps (26) and sister chromatid exchange (27). Although the precise mechanism inducing chromosome aberration by ITP or IDP is not known, exposure to a high concentration of ITP or IDP might also result in an increase of dI in nuclear DNA, thus increasing SSBs and chromosome abnormalities as observed in *Itpa*$^{-/-}$ primary MEFs. Moreover, both ITPA deficiency and exposure to ITP or IDP increase premature centromere separation (26). Increased inosine levels in cellular RNA prepared from *Itpa*$^{-/-}$ embryos indicated that the ITP level was also significantly increased in the absence of ITPA. Therefore, these chromosomal abnormalities might be caused by the increased level of ITP in nucleotide pool. Because sister chromatid cohesion is established by a cohesin complex composed of Rad21, Smc1α, Smc3 and two Scc3 orthologs, SA1 and SA2 (28,29) and whose reaction requires ATP, ITP might compete with ATP to disrupt sister chromatid cohesion, thus resulting in premature centromere separation and inappropriate chromatid separation.

Increased expression of *Nudt16* suppresses the ITPA-deficient phenotype during immortalization

During immortalization of *Itpa*$^{-/-}$ MEFs, most of the ITPA-deficient phenotype characteristics, such as prolonged doubling time, G2/M arrest, SSBs accumulation, chromosome abnormalities were canceled efficiently. This was accompanied by a significant reduction of dI accumulation in nuclear DNA. The inosine level in cellular RNA was still high in immortalized *Itpa*$^{-/-}$ MEFs (516.8 ± 22.3 inosine residues per 10^6 guanosine residues) as much as seen in *Itpa*$^{-/-}$ embryos (567.3 ± 41.4 inosine residues per 10^6 guanosines), thereby indicating that the ITPA-deficient phenotypes are most likely to be attributed to the increased accumulation of dI in nuclear DNA.

We identified the human NUDT16 protein (Iyama *et al.*, manuscript in preparation) as a dIDP/IDP-hydrolyzing enzyme, which can bind ITP/XTP/GTP and efficiently hydrolyzes dIDP/IDP, and to a lesser extent dITP/ITP, to dIMP/IMP. In the present study, we found that the levels of mouse *Nudt16* mRNA and NUDT16 protein were significantly higher in immortalized *Itpa*$^{-/-}$ MEFs than in immortalized wild-type MEFs or primary *Itpa*$^{-/-}$ MEFs. Because knockdown of *Nudt16* expression efficiently reproduced the ITPA-deficient phenotypes accompanied by significant increases of dI in nuclear DNA, and to a lesser extent of inosine in cellular RNA, we conclude that NUDT16 and ITPA play a dual protective role for eliminating dITP/ITP and dIDP/IDP from nucleotide pools in mammals.

ITP can be hydrolyzed slowly to IDP by ATPase or other nucleoside triphosphatases (11,30), so increased

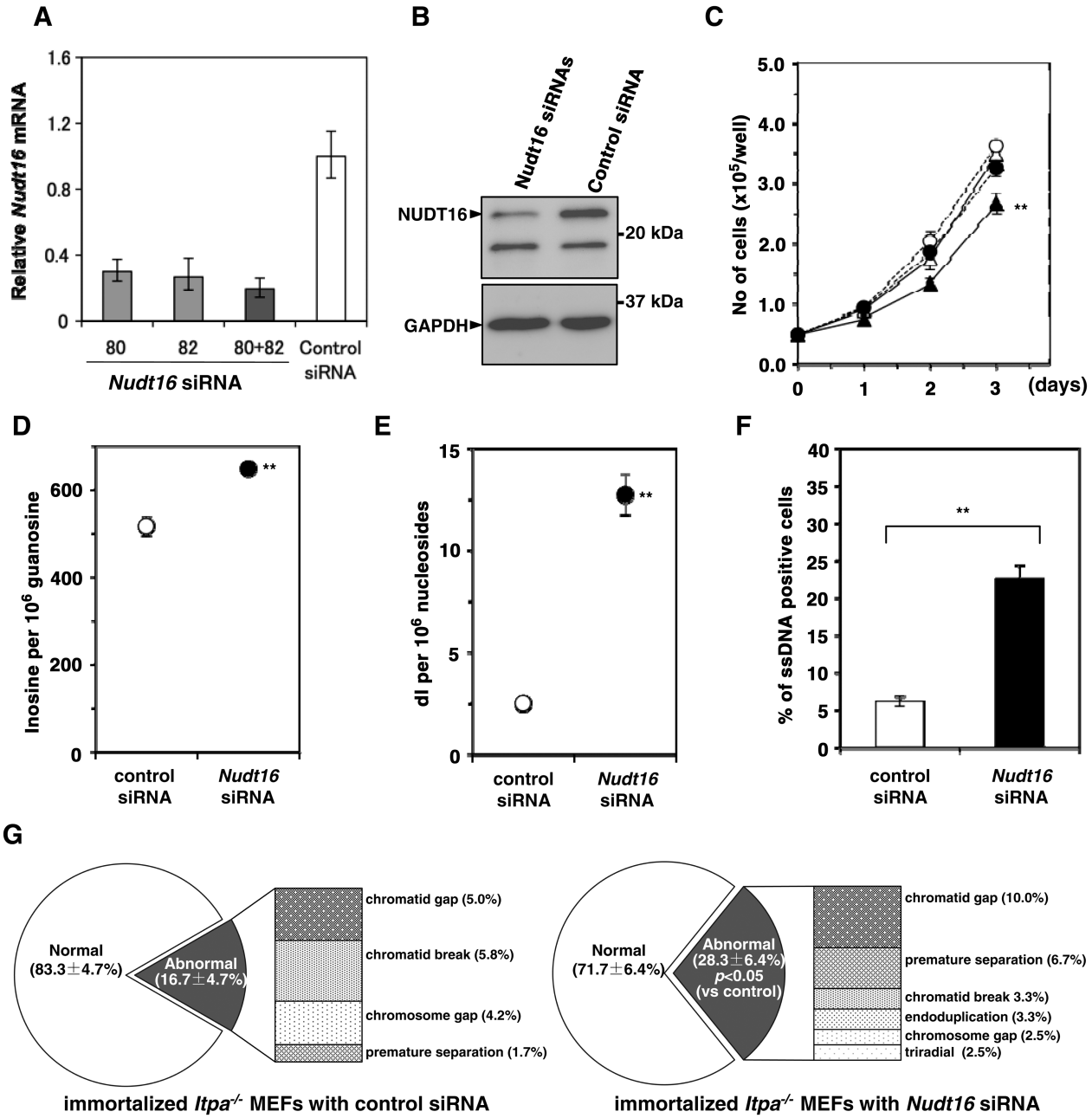

Figure 7. Knockdown of *Nudt16* mRNA suppressed ITPA-deficient phenotypes in immortalized $Itpa^{-/-}$ MEFs. (**A**) Expression of *Nudt16* mRNA. To knock down the expression of *Nudt16*, two different siRNAs (80, 82 or 80 + 82) against *Nudt16* mRNA or control siRNA were introduced into immortalized $Itpa^{-/-}$ MEFs. Forty-eight hours after the introduction, total RNA was prepared and quantitative real-time RT–PCR was performed. Levels of *Nudt16* mRNA were normalized to those of *Gapdh* mRNA and their relative values are shown. Data are shown in a bar graph (mean ± SD, $n = 3$). (**B**) Expression of NUDT16 protein. Western blotting was performed for crude cell extracts (40 μg) prepared from immortalized $Itpa^{-/-}$ MEFs treated with two *Nudt16* siRNAs (80 + 82) or control siRNA, using anti-NUDT16. GAPDH was detected as an internal control. (**C**) Knockdown of *Nudt16* mRNA suppressed proliferation of immortalized $Itpa^{-/-}$ MEFs. Expression of *Nudt16* mRNA was blocked using a mix of two different *Nudt16* siRNAs and cell proliferation was examined. Circles, $Itpa^{+/+}$; triangles, $Itpa^{-/-}$; open marks, control siRNA; closed marks, *Nudt16* siRNAs. Result of repeated measures ANOVA, two-tailed, $P < 0.0001$; Bonferroni/Dunn *post hoc* test, $^{**}P < 0.01$ (versus other three measures). Error bars represent the SD ($n = 4$). (**D**) Knockdown of *Nudt16* mRNA significantly increased the accumulation of inosine in RNA of immortalized $Itpa^{-/-}$ MEFs. Level of inosine in RNA was determined by LC–MS/MS analysis of RNA prepared from immortalized $Itpa^{-/-}$ MEFs treated with control or *Nudt16* siRNAs. Result of unpaired Student's *t*-test (two-tailed), $^{**}P < 0.01$. Data are shown as a bar graph with the mean ± SD ($n = 3$). (**E**) Knockdown of *Nudt16* mRNA significantly increased the accumulation of dI in nuclear DNA of immortalized $Itpa^{-/-}$ MEFs. Level of dI in nuclear DNA was determined by LC–MS/MS analysis of nuclear DNA prepared from immortalized $Itpa^{-/-}$ MEFs treated with control or *Nudt16* siRNAs. Result of unpaired Student's *t*-test (two-tailed), $^{**}P < 0.01$. Data are shown as a bar graph with the mean ± SD ($n = 3$). (**F**) Increased immunoreactivity against ssDNA in immortalized $Itpa^{-/-}$ MEFs after *Nudt16* knockdown. Immunofluorescence microscopy with anti-ssDNA antibody revealed significantly increased immunoreactivity after *Nudt16* knockdown. Result of unpaired Student's *t*-test (two-tailed), $^{**}P < 0.01$. Data are shown as a bar graph with the mean ± SD ($n = 4$). (**G**) Knockdown of *Nudt16* mRNA increased chromosomal abnormalities in immortalized $Itpa^{-/-}$ MEFs. The frequency of chromosomal abnormalities was increased significantly in immortalized $Itpa^{-/-}$ MEFs after *Nudt16* knockdown. Result of unpaired Student's *t*-test (two-tailed), $P < 0.05$ (versus control siRNA). Data are shown as pie charts with the mean ± SD ($n = 4$).

dIDP hydrolysis in immortalized *Itpa*$^{-/-}$ MEFs is likely to be sufficient to eliminate dITP from the nucleotide pools. Moreover, ITP can be generated in a variety of tissue extracts as well as in erythrocytes (31). We reported previously that ITP accumulated in erythrocytes but not in tissues including the heart and liver derived from *Itpa*$^{-/-}$ mice, whereas IMP accumulated markedly in RNA prepared from the latter (6). Because both RNA and DNA synthesis takes place in the latter tissues, DNA and RNA polymerases are likely to utilize ITP and dITP efficiently as nucleotide precursors, thereby consuming most of the ITP or dITP that accumulates in the nucleotide pools in the absence of ITPA.

Considering the likely source of ITP or dITP in the nucleotide pools, IMP generated from AMP by AMP deamination must be the most relevant precursor, because most cells can synthesize IDP or ITP from IMP (31) and IDP may be converted to dIDP by ribonucleotide reductase, thus generating dITP (21). To minimize accumulation of ITP or dITP in the nucleotide pools, hydrolysis of IDP or dIDP to the corresponding monophosphates catalyzed by NUDT16 is likely to be as critical as is any hydrolysis of ITP or dITP to the corresponding monophosphates.

In the present study, we showed that increased expression of NUDT16 in *Itpa*$^{-/-}$ immortalized MEFs is sufficient to cancel the ITPA-deficient phenotypes observed in *Itpa*$^{-/-}$ embryos or primary MEFs, suggesting that the lower expression level of NUDT16 in normal tissues may be why any ITPA deficiency causes such severe phenotypes. On the other hand, ITPA deficiency in humans is likely to be related to azathioprine intolerance in patients with inflammatory bowel disease, but does not cause any severe phenotype (32–34), compared with the *Itpa*$^{-/-}$ mice. It is possible that human NUDT16 expression might be higher than that in mouse, thus compensating for any ITPA deficiency.

Identification of NUDT16 as a backup enzyme for ITPA deficiency in mice will shed light on the mechanisms that enable humans to be resistant to ITPA deficiency. Towards this goal, it is important to know the relative expression of ITPA and NUDT16 in human cells and organs, and to characterize the enzymatic properties of NUDT16.

SUPPLEMENTARY DATA

Supplementary Data are available at NAR Online.

ACKNOWLEDGEMENTS

The authors thank M. Ohtsu in the Laboratory for Technical Support of our institute and N. Adachi, A. Matsuyama, K. Hayashi, K. Nakabeppu and K. Asakawa for technical assistance.

FUNDING

Ministry of Education, Culture, Sports, Science and Technology of Japan [20013034 to Y.N., 20012038 to K.S.]; the Japan Society for the Promotion of Science [19390114 to D.T., 08J03650 to T.I.]; Kyushu University Global COE program [YN]. Funding for open access charges: Ministry of Education, Culture, Sports, Science and Technology of Japan; Kyushu University Global COE program.

Conflict of interest statement. None declared.

REFERENCES

1. Nakabeppu,Y., Tsuchimoto,D., Furuichi,M. and Sakumi,K. (2004) The defense mechanisms in mammalian cells against oxidative damage in nucleic acids and their involvement in the suppression of mutagenesis and cell death. *Free Radic. Res.*, **38**, 423–429.
2. Nakabeppu,Y., Behmanesh,M., Yamaguchi,H., Yoshimura,D. and Sakumi,K. (2007) In Evans,M.D. and Cooke,M.S. (eds), *Oxidative Damage to Nucleic Acids*. Landes Bioscience/Springer, Austin, TX/New York, pp. 40–53.
3. Nakabeppu,Y. (2001) Molecular genetics and structural biology of human MutT homolog, MTH1. *Mutat. Res.*, **477**, 59–70.
4. Nakabeppu,Y., Kajitani,K., Sakamoto,K., Yamaguchi,H. and Tsuchimoto,D. (2006) MTH1, an oxidized purine nucleoside triphosphatase, prevents the cytotoxicity and neurotoxicity of oxidized purine nucleotides. *DNA Rep.*, **5**, 761–772.
5. Behmanesh,M., Sakumi,K., Tsuchimoto,D., Torisu,K., Ohnishi-Honda,Y., Rancourt,D.E. and Nakabeppu,Y. (2005) Characterization of the structure and expression of mouse *Itpa* gene and its related sequences in the mouse genome. *DNA Res.*, **12**, 39–51.
6. Behmanesh,M., Sakumi,K., Abolhassani,N., Toyokuni,S., Oka,S., Ohnishi,Y.N., Tsuchimoto,D. and Nakabeppu,Y. (2009) ITPase-deficient mice show growth retardation and die before weaning. *Cell Death Differ.*, **16**, 1315–1322.
7. Nonaka,M., Tsuchimoto,D., Sakumi,K. and Nakabeppu,Y. (2009) Mouse RS21-C6 is a mammalian 2′-deoxycytidine 5′-triphosphate pyrophosphohydrolase that prefers 5-iodocytosine. *FEBS J.*, **276**, 1654–1666.
8. Tsuzuki,T., Egashira,A., Igarashi,H., Iwakuma,T., Nakatsuru,Y., Tominaga,Y., Kawate,H., Nakao,K., Nakamura,K., Ide,F. *et al.* (2001) Spontaneous tumorigenesis in mice defective in the *MTH1* gene encoding 8-oxo-dGTPase. *Proc. Natl Acad. Sci. USA*, **98**, 11456–11461.
9. Shenoy,T.S. and Clifford,A.J. (1975) Adenine nucleotide metabolism in relation to purine enzymes in liver, erythrocytes and cultured fibroblasts. *Biochim. Biophys. Acta*, **411**, 133–143.
10. Gower,W.R. Jr, Carr,M.C. and Ives,D.H. (1979) Deoxyguanosine kinase. Distinct molecular forms in mitochondria and cytosol. *J. Biol. Chem.*, **254**, 2180–2183.
11. Burton,K., White,H. and Sleep,J. (2005) Kinetics of muscle contraction and actomyosin NTP hydrolysis from rabbit using a series of metal-nucleotide substrates. *J. Physiol.*, **563**, 689–711.
12. Bradshaw,J.S. and Kuzminov,A. (2003) RdgB acts to avoid chromosome fragmentation in *Escherichia coli*. *Mol. Microbiol.*, **48**, 1711–1725.
13. Ide,Y., Tsuchimoto,D., Tominaga,Y., Nakashima,M., Watanabe,T., Sakumi,K., Ohno,M. and Nakabeppu,Y. (2004) Growth retardation and dyslymphopoiesis accompanied by G2/M arrest in APEX2-null mice. *Blood*, **104**, 4097–4103.
14. Tsuruya,K., Furuichi,M., Tominaga,Y., Shinozaki,M., Tokumoto,M., Yoshimitsu,T., Fukuda,K., Kanai,H., Hirakata,H., Iida,M. *et al.* (2003) Accumulation of 8-oxoguanine in the cellular DNA and the alteration of the OGG1 expression during ischemia-reperfusion injury in the rat kidney. *DNA Rep.*, **2**, 211–229.
15. Taghizadeh,K., McFaline,J.L., Pang,B., Sullivan,M., Dong,M., Plummer,E. and Dedon,P.C. (2008) Quantification of DNA damage products resulting from deamination, oxidation and reaction with products of lipid peroxidation by liquid chromatography isotope dilution tandem mass spectrometry. *Nat. Protoc.*, **3**, 1287–1298.

16. Oka,S., Ohno,M., Tsuchimoto,D., Sakumi,K., Furuichi,M. and Nakabeppu,Y. (2008) Two distinct pathways of cell death triggered by oxidative damage to nuclear and mitochondrial DNAs. *EMBO J.*, **27**, 421–432.
17. Tsuchimoto,D., Sakai,Y., Sakumi,K., Nishioka,K., Sasaki,M., Fujiwara,T. and Nakabeppu,Y. (2001) Human APE2 protein is mostly localized in the nuclei and to some extent in the mitochondria, while nuclear APE2 is partly associated with proliferating cell nuclear antigen. *Nucleic Acids Res.*, **29**, 2349–2360.
18. Kow,Y.W. (2002) Repair of deaminated bases in DNA. *Free Radic. Biol. Med.*, **33**, 886–893.
19. Dalhus,B., Arvai,A.S., Rosnes,I., Olsen,Ø., Backe,P.H., Alseth,I., Gao,H., Cao,W., Tainer,J.A. and Bjørås,M. (2009) Structures of endonuclease V with DNA reveal initiation of deaminated adenine repair. *Nat. Struct. Mol. Biol.*, **16**, 138–143.
20. Karran,P. and Lindahl,T. (1978) Enzymatic excision of free hypoxanthine from polydeoxynucleotides and DNA containing deoxyinosine monophosphate residues. *J. Biol. Chem.*, **253**, 5877–5879.
21. Myrnes,B., Guddal,P.H. and Krokan,H. (1982) Metabolism of dITP in HeLa cell extracts, incorporation into DNA by isolated nuclei and release of hypoxanthine from DNA by a hypoxanthine-DNA glycosylase activity. *Nucleic Acids Res.*, **10**, 3693–3701.
22. Saparbaev,M. and Laval,J. (1994) Excision of hypoxanthine from DNA containing dIMP residues by the *Escherichia coli*, yeast, rat, and human alkylpurine DNA glycosylases. *Proc. Natl Acad. Sci. USA*, **91**, 5873–5877.
23. Moe,A., Ringvoll,J., Nordstrand,L.M., Eide,L., Bjørås,M., Seeberg,E., Rognes,T. and Klungland,A. (2003) Incision at hypoxanthine residues in DNA by a mammalian homologue of the *Escherichia coli* antimutator enzyme endonuclease V. *Nucleic Acids Res.*, **31**, 3893–3900.
24. Vallur,A.C., Maher,R.L. and Bloom,L.B. (2005) The efficiency of hypoxanthine excision by alkyladenine DNA glycosylase is altered by changes in nearest neighbor bases. *DNA Rep.*, **4**, 1088–1098.
25. Pardo,B., Gómez-González,B. and Aguilera,A. (2009) DNA double-strand break repair: how to fix a broken relationship. *Cell. Mol. Life Sci.*, **66**, 1039–1056.
26. Auclair,C., Gouyette,A., Levy,A. and Emerit,I. (1990) Clastogenic inosine nucleotide as components of the chromosome breakage factor in scleroderma patients. *Arch. Biochem. Biophys.*, **278**, 238–244.
27. Vormittag,W. and Brannath,W. (2001) As to the clastogenic-, sister-chromatid exchange inducing-and cytotoxic activity of inosine triphosphate in cultures of human peripheral lymphocytes. *Mutat. Res.*, **476**, 71–81.
28. Watrin,E. and Peters,J.M. (2006) Cohesin and DNA damage repair. *Exp. Cell Res.*, **312**, 2687–2693.
29. Uhlmann,F. (2009) A matter of choice: the establishment of sister chromatid cohesion. *EMBO Rep.*, **10**, 1095–1102.
30. Vanderheiden,B.S. (1975) ITP pyrophosphohydrolase and IDP phosphohydrolase in rat tissue. *J. Cell. Physiol.*, **86**, 167–175.
31. Vanderheiden,B.S. (1979) Inosine di- and triphosphate synthesis in erythrocytes and cell extracts. *J. Cell. Physiol.*, **99**, 287–301.
32. Sumi,S., Marinaki,A.M., Arenas,M., Fairbanks,L., Shobowale-Bakre,M., Rees,D.C., Thein,S.L., Ansari,A., Sanderson,J., De Abreu,R.A. *et al.* (2002) Genetic basis of inosine triphosphate pyrophosphohydrolase deficiency. *Hum. Genet.*, **111**, 360–367.
33. Marinaki,A.M., Duley,J.A., Arenas,M., Ansari,A., Sumi,S., Lewis,C.M., Shobowale-Bakre,M., Fairbanks,L.D. and Sanderson,J. (2004) Mutation in the ITPA gene predicts intolerance to azathioprine. *Nucleosides Nucleotides Nucleic Acids*, **23**, 1393–1397.
34. Seela,F. and Xu,K. (2007) Pyrazolo[3,4-*d*]pyrimidine ribonucleosides related to 2-aminoadenosine and isoguanosine: synthesis, deamination and tautomerism. *Org. Biomol. Chem.*, **5**, 3034–3045.